BJP | BRITISH PHARMACOLOGICAL SOCIETY

Small molecule-facilitated anion transporters in cells for a novel therapeutic approach to cystic fibrosis

Michele Fiore[1] | Claudia Cossu[1] | Valeria Capurro[2] | Cristiana Picco[1] |
Alessandra Ludovico[1] | Marcin Mielczarek[3] | Israel Carreira-Barral[3] | Emanuela Caci[2] |
Debora Baroni[1] | Roberto Quesada[3] | Oscar Moran[1] (ID)

[1] Istituto di Biofisica, CNR, Genova, Italy

[2] U.O.C. Genetica Medica, Istituto Giannina Gaslini, Genova, Italy

[3] Departamento de Química, Facultad de Ciencias, Universidad de Burgos, Burgos, Spain

Correspondence
Oscar Moran, Istituto di Biofisica, CNR, via De Marini, 6 16149 Genova, Italy.
Email: oscar.moran@cnr.it

Funding information
European Union's Horizon 2020 research and innovation programme, Grant/Award Number: No. 667079

Background and Purpose: Cystic fibrosis (CF) is a lethal autosomal recessive genetic disease that originates from the defective function of the CF transmembrane conductance regulator (CFTR) protein, a cAMP-dependent anion channel involved in fluid transport across epithelium. Because small synthetic transmembrane anion transporters (anionophores) can replace the biological anion transport mechanisms, independent of genetic mutations in the CFTR, such anionophores are candidates as new potential treatments for CF.

Experimental Approach: In order to assess their effects on cell physiology, we have analysed the transport properties of five anionophore compounds, three prodigiosines and two tambjamines. Chloride efflux was measured in large uni-lamellar vesicles and in HEK293 cells with chloride-sensitive electrodes. Iodide influx was evaluated in FRT cells transfected with iodide-sensitive YFP. Transport of bicarbonate was assessed by changes of pH after a NH_4^+ pre-pulse using the BCECF fluorescent probe. Assays were also carried out in FRT cells permanently transfected with wild type and mutant human CFTR.

Key Results: All studied compounds are capable of transporting halides and bicarbonate across the cell membrane, with a higher transport capacity at acidic pH. Interestingly, the presence of these anionophores did not interfere with the activation of CFTR and did not modify the action of lumacaftor (a CFTR corrector) or ivacaftor (a CFTR potentiator).

Conclusion and Implications: These anionophores, at low concentrations, transported chloride and bicarbonate across cell membranes, without affecting CFTR function. They therefore provide promising starting points for the development of novel treatments for CF.

1 | INTRODUCTION

Cystic fibrosis (CF) is the most common, autosomal recessive, lethal genetic disease in the Caucasian population (Bobadilla, Macek, Fine,

& Farrell, 2002; Strausbaugh & Davis, 2007). The major cause of CF morbidity and mortality is lung dysfunction, characterised by infection, inflammation, and airway damage, leading to respiratory failure. More than 2,000 mutations in the CF transmembrane

conductance regulator (CFTR), classified in six classes according to the effect of the mutation, lead to anion transport defects in epithelium by various mechanisms (failure to synthesise the protein, processing flaws, gating or conductance defects, and reduced expression; Castellani & Assael, 2017). The F508del mutation of the CFTR protein underlies most CF cases, causing a defective trafficking to the plasma membrane (class II mutation) and reduced activity of the channel preventing CFTR from undertaking its normal function (class III mutation). Efforts have been made to restore CFTR function by gene therapy or by using small (low MW) organic compounds to ameliorate the disease (Galietta, 2013; Hudock & Clancy, 2017; Zegarra-Moran & Galietta, 2017). To address the reduced activity defect of G551D (class III mutations) and of other less frequent mutations the potentiator, ivacaftor, which improves chloride transport and lung function of patients, has been introduced (Ramsey et al., 2011). However, attempts to enhance chloride transport by using drugs that increase delivery of functional F508del-CFTR to the cell surface have been less successful. Lumacaftor, a CFTR corrector, increased the cell surface density of functional F508del-CFTR in vitro (Ren et al., 2013; Van Goor et al., 2011; Zegarra-Moran & Galietta, 2017) but has a very modest beneficial effects in patients (Boyle et al., 2014; Clancy et al., 2012; De Boeck & Davies, 2017; Wainwright et al., 2015). CF patients treated with a new corrector, tezacaftor, in combination with lumacaftor and ivacaftor, have shown a promising moderate amelioration (Davies et al., 2018)

An alternative strategy could be the use of molecules capable of transporting anions across lipid bilayers, termed anionophores, to substitute the dysfunctional transport in CF. In this regard, although several studies have been published recently, functional analyses of this type of compound in cells are still very limited (Cossu et al., 2018; Davis, Okunola, & Quesada, 2010; Dias et al., 2018; Hernando, Soto-Cerrato, Cortés-Arroyo, Pérez-Tomás, & Quesada, 2014; Li et al., 2016; Li, Salomon, Sheppard, Mall, & Galietta, 2017; Valkenier et al., 2014; Wu et al., 2016). The idea of using anionophores to replace the defective CFTR protein has the advantage of providing a general therapy for CF that would be independent of the specific mutation.

With this perspective, we have synthetised and characterised the transport properties of five anionophores. We have studied the natural product prodigiosine (PRG; Rapoport & Holden, 1962), the synthetic derivative obatoclax (OBX; Díaz de Greñu et al., 2011), the triazole derivative of prodigiosine, EH130 (Hernando et al., 2018), and two synthetic analogues of the marine alkaloids (tambjamines), RQ363 (Hernando, Soto-Cerrato, Cortés-Arroyo, Pérez-Tomás, & Quesada, 2014) and MM3. The last three compounds, EH130, RQ363, and MM3, are interesting because they retain a significant anion transport capacity but have reduced cytotoxicity. Here, we show that these anionophores are able to transport relevant anions physiologically, such as chloride and bicarbonate, in mammalian cells, without a significant interference with the transport and pharmacology of existing CFTR, either native or treated with drugs.

What is already known
- The anion channel CFTR is defective in cystic fibrosis.

What this study adds
- Anionophores are small molecules able to efficiently transport halides and bicarbonate across cell membranes.
- Anionophores do not interfere with the function and pharmacology of CFTR.

What is the clinical significance
- Anionophores could be used as substitution therapy in cystic fibrosis.

2 | METHODS

2.1 | Synthesis of the anionophores

Anionophores PRG (Rapoport & Holden, 1962), OBX (Díaz de Greñu et al., 2011), EH130 (Hernando et al., 2018), and RQ3634 (Hernando, Soto-Cerrato, Cortés-Arroyo, Pérez-Tomás, & Quesada, 2014) were synthesised as previously reported (see Figure 1a). MM3 was prepared by reaction of 3-ethyl-4-methyl-1H,1′H-[2,2′-bipyrrole]-5-carbaldehyde (250.9 mg, 1.24 mmol) with glacial acetic acid (50 μl) and cyclohexylamine (275 μl, 2.40 mmol, 1.94 equiv.) in chloroform (10 ml). The reaction mixture was stirred at 60°C for 6 hr. Upon cooling to room temperature, the chloroform was evaporated under reduced pressure, and the residue was re-dissolved in dichloromethane (30 ml). The solution of the crude compound MM3 was washed with 1 M aqueous HCl solution (3 × 20 ml), dried over anhydrous Na_2SO_4, filtered, and evaporated to dryness under reduced pressure. The residue was re-crystallised from a mixture of dichloromethane and n-hexane to give compound MM3 as dark yellow needles (yield: 264.2 mg, 67%). All compounds were fully characterised by MS and NMR. Detailed characterisation is provided in the Supporting Information. Purities of compounds were estimated by ^{1}H NMR to be greater than 96% for all tested compounds. Except when indicated, all other chemicals were purchased from Sigma-Aldrich. The chemical structures of the studied compounds are shown in Figure 1a.

2.2 | Chloride efflux in phospholipid large uni-lamellar vesicles

The activity of the transmembrane carriers was assayed in model 1-palmitoyl-2-oleoyl-sn-glycero-3-phosphocholine large uni-lamellar vesicles (LUVs) with an average diameter of 200 nm as described elsewhere (Cossu et al., 2018; Hernando et al., 2018; Soto-Cerrato et al., 2015). LUVs were prepared by extrusion across polycarbonate membranes (LiposoFast Basic extruder; Avestin, Inc.). LUVs were prepared in a high chloride solution (489 mM NaCl and 5 mM phosphate buffer,
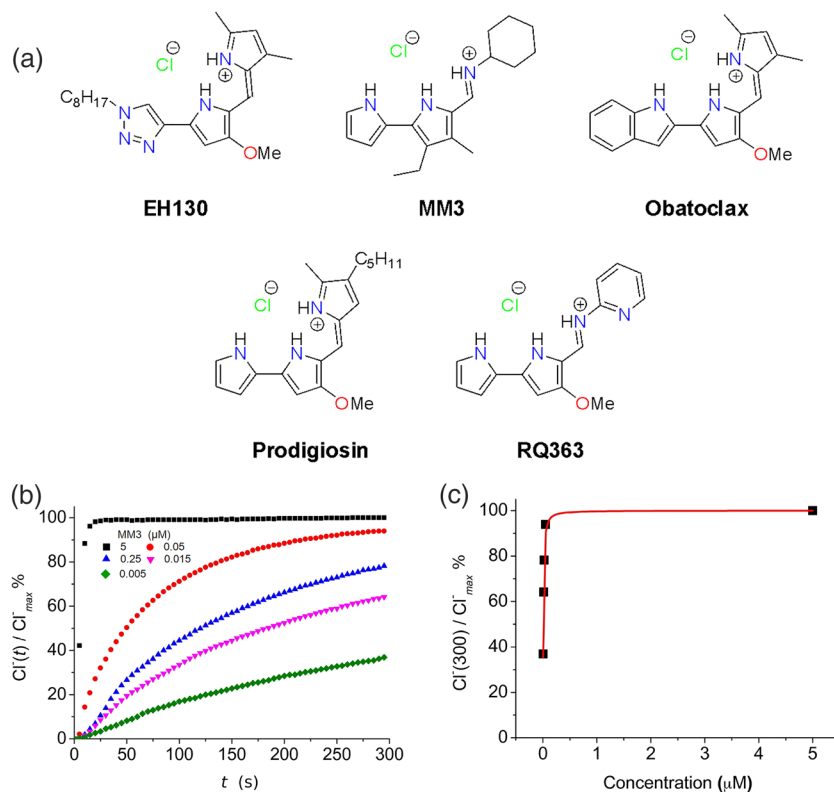
FIGURE 1 (a) Chemical structures of the studied compounds. (b) Chloride efflux promoted by MM3 at different concentrations (5 μM, 0.05 μM; 0.025 μM, 0.015 μM, 0.005 μM) in LUV. Vesicles loaded with 489 mM NaCl were buffered at pH 7.2 with 5 mM phosphate and dispersed in 489 mM $NaNO_3$ buffered at pH 7.2. Each trace represents the average of three independent measurements. (c) The normalised chloride efflux at 300 s plotted against the anionophore concentration. The dose–response curve was constructed from 15 independent measurements. Data have been fitted with Hill equation (continuous line), which yields an EC_{50} of 0.0083 μM

pH 7.2) and dialyzed against a nitrate solution (489 mM $NaNO_3$ and 5 mM phosphate buffer, pH 7.2) to remove the unencapsulated chloride. Final concentration of 1-palmitoyl-2-oleoyl-sn-glycero-3-phosphocholine in the experiments was 0.5 mM. The chloride efflux from chloride-loaded LUV was monitored, recording the time course of the external chloride concentration using ion selective electrodes (Vernier, Beaverton, Oregon, USA, or Hach Chloride Ion Selective Electrode, Loveland, Colorado, USA). Both chloride-sensitive electrodes used have a measuring range from 1 mg·L^{-1} to 35 g·L^{-1} and a linear response (voltage vs. log concentration) of 55 ± 4 mV per decade at 20 ± 5°C. Release of all encapsulated chloride by addition of detergent allows the normalisation of the data. The anionophore activity was expressed as the normalised concentration released after 300 s. The relative potency of the anionophore transport was estimated as the concentration to induce 50% of the maximum chloride release in time interval.

2.3 | Cell viability and apoptosis

Cell toxicity of anionophores was evaluated in HEK293 (CLS Cat# 300192/p777_HEK293, RRID:CVCL_0045), CHO (CLS Cat# 603479/p746_CHO, RRID:CVCL_0213), and Fischer rat thyroid (FRT) cells by the Trypan blue exclusion (Louis & Siegel, 2011). Cells were exposed to each compound for 30 min. After exposure, cells were trypsinised and harvested for toxicity evaluation. To avoid an underestimation of the amount of dead cells, also the cells that have been detached from the plate during the anionophore exposition were collected and assayed. For each cell line (CHO, FRT, and HEK293), the

concentrations of each compound that were assayed were 10, 5, 2.5, 2, 1, 0.5, 0.25, 0.125, 0.0625, and 0 (vehicle, DMSO) μM. For each cell line and for each concentration assayed, the toxic effect of anionophores was evaluated performing the Trypan blue test on five biological replicates. In each experiment, an amount of at least 150 cells was considered. The concentration to have half of the maximum toxicity, TD_{50}, was calculated plotting the percentage of cell survival against the anionophore concentration (A) and fitting the data with

$$\%survival = 100 \times \frac{TD_{50}}{TD_{50} + A}. \quad (1)$$

An assay to distinguish between healthy, early apoptotic, late apoptotic, and necrotic cells (Apoptosis/Necrosis Detection KitR, Enzo, Lausen, Switzerland) was applied to HEK293 cells treated with anionophores. HEK293 cells were exposed for 15 min to each compound, at concentrations of 1.5, 0.5, 0.25, or 0 μM. This assay is compatible with GFP and YFP fluorescent probes, but the fluorescence of prodigiosin and OBX interferes with the assay, vitiating the apoptosis test with these two anionophores. The maximum inducible apoptosis AD_{50} was calculated fitting the percentage of apoptotic cells against the anionophore concentration with an equation similar to that used for toxicity calculations.

2.4 | Chloride efflux assay using cells

HEK293 cells were grown in standard conditions (37°C, 5% CO_2), in DMEM medium supplemented with 2 mM L-glutamine and 10%

FBS. CHO cells were grown in standard conditions, in Ham's F12 medium supplemented with 2 mM L-glutamine and 10% FBS. Cells at 80% confluence were detached from the bottom of the flask by soft scraping, washed in chloride-free buffer (in mM: 136 NaNO$_3$, 3 KNO$_3$, 2 Ca (NO$_3$)$_2$, 20 HEPES, 11 glucose, pH 7.4), suspended in 4 ml of chloride-free buffer (~15 × 10^6 cells), and used immediately. Ionophores were dissolved in 100% DMSO to a concentration of 10 mM. The final concentration of DMSO cells were exposed was ≤0.3%. The vehicle control was application of 0.3% DMSO. Chloride concentration in the extracellular solution was continuously measured with the chloride-sensitive electrode (Cossu et al., 2018; Hernando et al., 2018). After an initial equilibration, chloride efflux was induced by a small volume (<1%) of ionophore. The measurement was concluded with the addition of SDS at a final concentration of 1% to lyse the cell membranes and measure the total chloride content in the cells. Experiments were carried out at 25 ± 1°C.

2.5 | Iodide influx assay using cells

FRT cells were stably transfected with a halide-sensitive yellow fluorescent protein (YFP-H148Q/I152L; Galietta et al., 2001; Galietta, Jayaraman, & Verkman, 2001). Cells were cultured in standard conditions (37°C, 5% CO$_2$) on black-wall, clear bottom 96-well micro-plates at a density of 40,000 cells per well in Coon's modified medium supplemented with 10% serum, 2 mM L-glutamine, 1 mg·ml^{-1} penicillin, 100 μg·ml^{-1} streptomycin, and 0.5 mg·ml^{-1} hygromycin as selection agent for the YFP. For some experiments, cells were stably co-transfected with the YFP and with a wild type CFTR, or CFTR carrying the CF mutations G551D or F508del . In these cases, the culture medium contained 1 mg·ml^{-1} geneticin (G418) and 0.6 mg·ml^{-1} zeocin as selection agents. Functional experiments were carried out 48 hr after cell seeding.

The activity of anionophores was determined in FRT cells expressing the halide-sensitive YFP protein, using a fluorescence plate reader (Tristar2 S, Berthold Technologies) equipped with 485 nm excitation and 535 nm emission filters, as previously described (Caci et al., 2008). The assay is based on the fact that the fluorescence of the YFP protein is quenched to a greater extend by I$^-$ than by Cl$^-$ (Galietta, Haggie, & Verkman, 2001). If not otherwise stated, 30 min before the assay, the cells were washed twice with a solution containing (in mM): NaCl 136, KNO$_3$ 4.5, Ca (NO$_3$)$_2$ 1.2, MgSO$_4$ 0.2, glucose 5, HEPES 20 (pH 7.4). The cells were incubated in 60 μl of this solution at 37°C with anionophores or with DMSO as control.

Once the assay had started, the fluorescence was recorded every 0.2 s for between 14 and 65 s for each well. At 5 s after the start of fluorescence recording, 100 μl of an extracellular solution containing 136 mM NaI instead of NaCl, were injected so that the final concentration of NaI in the well was 85 mM. The iodide influx was assessed as a quenching of fluorescence, as the anion binds to the intracellular YFP. The initial rate of fluorescence decay (QR) was derived by fitting the signal with a double exponential function, after background subtraction and normalisation for the average fluorescence before NaI

addition (Galietta, Haggie, & Verkman, 2001; Galietta, Jayaraman, & Verkman, 2001; Caci et al., 2008). The QR is a direct indication of the activity of the tested compound.

For the pH-dependence experiments, cells were washed with a solution containing (in mM): NaCl 137, KCl 2.7, Na$_2$HPO$_4$ 8.1, KH$_2$PO$_4$ 1.5, CaCl$_2$ 1, and MgCl$_2$ 0.5 (pH 7.3). During the assay, 165 μl of an extracellular solution containing 137 mM NaI instead of NaCl, were injected so that the final concentration of NaI in the well was 100 mM. To explore the effect of lowering the extracellular pH, the NaI solution was buffered at pH 6.9 with HEPES or at pH 6.6 and 6.2 using MES. The YFP fluorescence plate was measured with a plate reader (FLUOstar Galaxy, BMG) equipped with 500 nm excitation and 535 nm emission filters.

2.6 | Membrane potential measurements

Changes of the cell membrane potential were measured in HEK293 cells with the fluorescence probe bis-(1,3-dibutylbarbituric acid) trimethine oxonol (DiBAC$_4$(3), Thermo Fisher Scientific, Rodano, Italy), with an excitation wavelength at 485 nm and emission to 520 nm. With this probe, hyperpolarisation is observed as the decrease of fluorescence. HEK293 cells seeded on 96-well micro-plates at a density of 40,000 cells per well. Cells were incubated in 60 μl of Cl solution (in mM: NaCl 136, KNO$_3$ 4.5, Ca (NO$_3$)$_2$ 1.2, MgSO$_4$ 0.2, glucose 5, HEPES 20, pH 7.4) or in gluconate solution (Na-gluconate substituting the NaCl) with 1 μM of DiBAC$_4$(3) dye, with or without 2 μM of anionophores or DMSO as control (see Figure S12), for 30 min at 37°C in agitation. The final concentration of DMSO to which cells were exposed was ≤0.3% in all assays, both with anionophores and as vehicle. Cells were washed twice with 100 μl of the respective buffer, and fluorescence was measured in the plate reader. The change of the membrane potential in a given condition was expressed as the relative change of the probe DiBAC$_4$(3) fluorescence, normalised by the fluorescence of the untreated cells, kept in normal NaCl extracellular solution, as the resting membrane potential reference ($\Delta F / F_0$).

2.7 | Bicarbonate transport in cells

The intracellular pH (pH$_i$) was measured in FRT cells using the fluorescent pH indicator 2′,7′-bis(2-carboxyethyl)-5-(and-6)carboxyfluorescein (BCECF). FRT cells, seeded on glass-bottom petri dishes, and grown to ~80% confluence. Cells were loaded with 5 μM of BCECF acetoxymethyl ester in the culture medium without serum for 30–40 min at room temperature. Cells were washed three times with recording solution containing (mM): NaCl 140, K$_2$HPO$_4$ 2.5, MgSO$_4$ 1, CaCl$_2$ 1, HEPES 10, glucose 6 (pH 7.3) and were allowed to recover for at least 30 min before measurement. All solutions were equilibrated with 5% CO$_2$ and 95% air. The petri dish was mounted in a perfusion system in the stage of an optical instrument composed of a basic iMIC epifluorescence inverted microscope with a QImaging Retiga EXI Blue camera (Till Photonics, Graefelfing, Germany). Cells were visualised

with an Olympus Objective Plan Super Apochromat 10x (N.A. 0.4, W. D. 30.1 mm). For excitation, we used Till Oligochrome, a wavelength-switching device containing a stable Xenon light-source. Sample was excited at two wavelenghs, 440 and 490 nm, and emission was recorded at 520 nm. To estimate the pH_i, the pH_i was varied incubating the cells in a high potassium concentration solution with 15 μM nigericin to equilibrate external with internal pH; a calibration curve was constructed plotting the pH against the ratio of fluorescence emitted upon excitation at the two excitation wavelengths.

The transport of bicarbonate was examined measuring the changes of pH_i using the NH_4^+ prepulse technique (Kintner et al., 2004). NH_4^+ solutions were prepared by replacing 20 mM NaCl in the recording solution with an equimolar concentration of NH_4Cl. When cells were subjected to an acid load by the transient application (2–3 min) of a 20 mM NH_4^+ solution, pH_i rose as NH_4^+ accumulated in the intracellular space during the prepulse. Cells were subsequently returned to a recording solution without NH_4^+, and acidification of the cytoplasm occurred when NH_3 quickly diffused out of the cell. For the extracellular bicarbonate solution, 40 mM of NaCl was substituted by $NaHCO_3$. The **Na^+/H^+ exchange** and the **Na^+/HCO_3^- co-transport** were inhibited with 1 mM **amiloride**, and the **Cl^-/HCO_3^-** and the **Na^+-dependent Cl^-/HCO_3^- exchangers** inhibited by adding 300 μM disodium 4,4′-diisothiocyano-2,2′-stilbenedisulfonate (**DIDS**) to the recording solution (Burnham, Amlal, Wang, Shull, & Soleimani, 1997; Lee et al., 1999; Shumaker & Soleimani, 1999) Moreover, DIDS also inhibits the calcium-activated chloride channels bestrophin and **anoctamin 1** that both display HCO_3^- permeability (Hartzell, Putzier, & Arreola, 2005). Anionophores were added directly to the solution to the desired concentration. Similar experiments were carried out with FRT cells stably transfected with CFTR, and 20 μM forskolin was added to the recording solutions to activate CFTR channels.

2.8 | Drug interactions

FRT cells stably transfected with a halide-sensitive YFP and CFTR (wild type or the CFTR-mutants G551D and F508del) were plated on 96-well micro-plates as described above. The iodide influx assay was used to investigate the possible interference by anionophores, of the activity of drugs, potentiators, and correctors, which interact with CFTR. Cells expressing wild type CFTR were incubated for 40 min with selected anionophore as control and 20 μM of forskolin to activate CFTR transport and with or without 10 μM of the CFTR potentiator ivacaftor. Cells expressing the G551D CFTR mutant were incubated with the selected anionophore and 20 μM of forskolin, with or without 10 μM of the CFTR potentiator ivacaftor to activate G551D mutant (Eckford, Li, Ramjeesingh, & Bear, 2012; Gianotti et al., 2013; Hadida et al., 2014). Cells expressing F508del mutant were incubated overnight with 5 μM of lumacaftor (Loo & Clarke, 2017; Ren et al., 2013; Van Goor et al., 2011). For the assay, cells were incubated with 20 μM forskolin, with or without anionophores to measure anion transport. In all experiments, the vehicle DMSO was used as negative control.

2.9 | Data and statistical analysis

The data and statistical analysis comply with the recommendations on experimental design and analysis in pharmacology (Curtis et al., 2018) Data were analysed with IgorPro 7 (Lake Oswego, Oregon, USA). All values are presented as the mean ± SEM, and n represents the number of experiments. Data points were weighted by their SD in the fit of concentration–response curves. Fitting results are presented ±SD. Comparison between two groups and a group against a specified value was done using Student's t test (Zar, 1999), and the t, probability P, and degrees of freedom v values were calculated. All experiments were performed unblinded.

2.10 | Materials

Ivacaftor and lumacaftor were supplied by Selleck Chemicals (Munich, Germany); amiloride, DIDS and forskolin were supplied by Sigma-Aldrich (St. Louis, MO).

2.11 | Nomenclature of targets and ligands

Key protein targets and ligands in this article are hyperlinked to corresponding entries in http://www.guidetopharmacology.org, the common portal for data from the IUPHAR/BPS Guide to PHARMACOLOGY (Harding et al., 2018), and are permanently archived in the Concise Guide to PHARMACOLOGY 2017/18 (Alexander et al., 2017).

3 | RESULTS

3.1 | Anionophore-driven chloride transport in vesicles

The five selected compounds, PRG, OBX, EH130, MM3, and RQ363, were first assayed in phospholipid LUVs. All these compounds promoted the efflux of the chloride encapsulated in LUVs. Figure 1b displays the time course of the normalised chloride concentration upon the addition of MM3 at concentrations from 0.005 to 5 μM, showing that the chloride efflux depends on the concentration of the anionophore. Application of the vehicle (DMSO) did not produce any chloride efflux (Cossu et al., 2018; Hernando et al., 2018). Application of the anionophore elicited chloride release from the interior of the vesicles, raising the external chloride concentration, as detected by the chloride selective electrode. A maximum chloride concentration was obtained by lysing the vesicles with a detergent. This Cl^- max value is used for normalisation of the data. The initial time, $t = 0$, represents addition of the anionophore, and $t = 300$ s is the arbitrary time chosen to end the experiments. The dose–response was constructed plotting the normalised chloride efflux in 300 s against the anionophore concentration, and data were fitted with the Hill's equation (Figure 1c). The same procedure was applied to each of the studied anionophores (see Figures S7–S11), and the results of

the dose–response fittings are presented in Table 1. Prodigiosin is the most potent anionophore, while its triazole derivative EH130 is about sevenfold less potent (Hernando et al., 2018). Also, the two tambjamines studied exhibited different potencies, MM3 being 2.5-fold more potent than RQ363 (Hernando, Soto-Cerrato, Cortés-Arroyo, Pérez-Tomás, & Quesada, 2014). For all anionophores, the Hill's exponent was not significantly different from 1, suggesting that the molecules participate in the transport as monomers (Black & Leff, 1983; Weiss, 1997).

3.2 | Anionophore toxicity

Toxicity data for the cell lines CHO, FRT, and HEK293 are presented in Table 2. The concentration for 50% of the maximum toxicity, TD_{50}, is quite well correlated in the three cell lines, showing that OBX and PRG are the most toxic substances. As previously described, EH130, the triazole derivative of prodigiosine, attenuates the cell toxicity of the anionophore (Cossu et al., 2018; Hernando et al., 2018), while the two tambjamines are significantly less toxic than prodigiosines. The concentrations to obtain the half of the maximum inducible apoptosis are also shown in Table 2. For all evaluated data,

TABLE 1 Relative potencies of the anionophores tested

Compound	EC_{50} (nM)	α
EH130	18.2 ± 1	1.17 ± 0.08
Obatoclax	9.7 ± 0.3	1.21 ± 0.06
Prodigiosin	2.5 ± 0.03	1.1 ± 0.11
MM3	8.3 ± 0.7	1.2 ± 0.012
RQ363	21.4 ± 9	0.9 ± 0.3

The effect of the anionophores was measured as normalised chloride efflux in 300 s, from large unilamelar vesicles. EC_{50} is the concentration for 50% of the maximum efflux, and α is the Hill's exponent of the dose–response curve. Data were obtained from the fit (±SEM) of dose–response curves constructed from ≥15 independent measurements.

TABLE 2 Effect of anionophores on cell viability

| | CHO | FRT | HEK293 | |
Compound	TD_{50} (μM)	TD_{50} (μM)	TD_{50} (μM)	AD_{50} (μM)
EH130	8.0 ± 0.6	9.0 ± 1.1	6.2 ± 0.4	2.4 ± 0.1
Obatoclax	5.6 ± 0.6	4.1 ± 0.6	3.7 ± 0.4	—
Prodigiosin	7.0 ± 0.6	3.9 ± 0.8	2.9 ± 0.34	—
MM3	16.8 ± 2.1	22.2 ± 4.4	24.7 ± 3.2	3.7 ± 0.9
RQ363	18.0 ± 3.2	22.2 ± 3.0	17.1 ± 1.2	12.6 ± 0.6

Viability of CHO, FRT and HEK293 cells was assessed by Trypan blue exclusion, after 30 min incubation with anionophore. TD_{50} (±SEM) is the concentration for 50% of the maximum toxicity. The concentration for the 50% of maximum inducible apoptosis is AD_{50}. Data shown are means±SEM from five independent experiments.

extrapolation to high anionophore concentrations indicates that all could induce 100% apoptosis.

## 3.3 | Chloride efflux assay in cells

We measured the anionophore-driven chloride efflux on suspensions of HEK293 or CHO cells. Application of the anionophore vehicle, DMSO, did not induce any measurable chloride efflux (Figure S12). By contrast, addition of micromolar concentrations of anionophores evoked a significant efflux of chloride ions from the cells, as shown in Figure 2. Application of EH130 (Figure 2a) and MM3 (Figure 2b) induced a concentration-dependent chloride efflux and similar effects were produced when the anionophores PRG, OBX, and RQ363 were added to cell suspensions (Figure S12). Cell responses were similar with the two cell lines, HEK293 and CHO cells. These experiments provided qualitative information and to acquire quantitative data, the iodide influx assay was used (see below).

3.4 | Iodide influx assay in cells

The iodide influx was measured as the initial quenching rate of the fluorescence in FRT cells expressing iodide-sensitive YFP. Figure 3a shows the time course of the fluorescence decay after addition of iodide to the extracellular solution. Control cells, treated with the vehicle DMSO, showed a slow quenching rate, QR, consistent with the endogenous transport of iodide by FRT cells. Treatment of cells
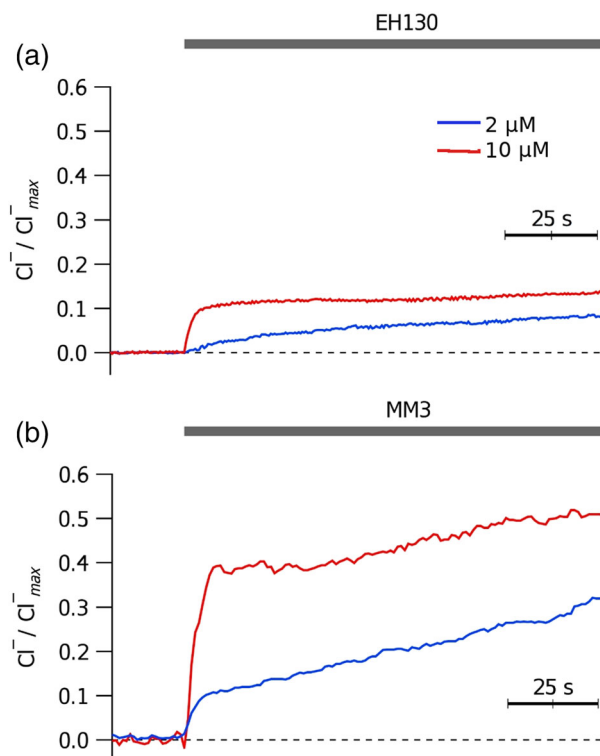
FIGURE 2 Chloride efflux measured in CHO cells upon addition of different concentrations of EH130 (a) and MM3 (b). The application of 2 μM or 10 μM of the anionophores are indicated by the upper bar
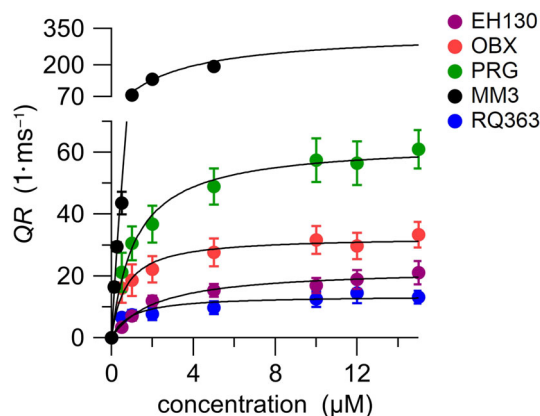
(a)

(b)
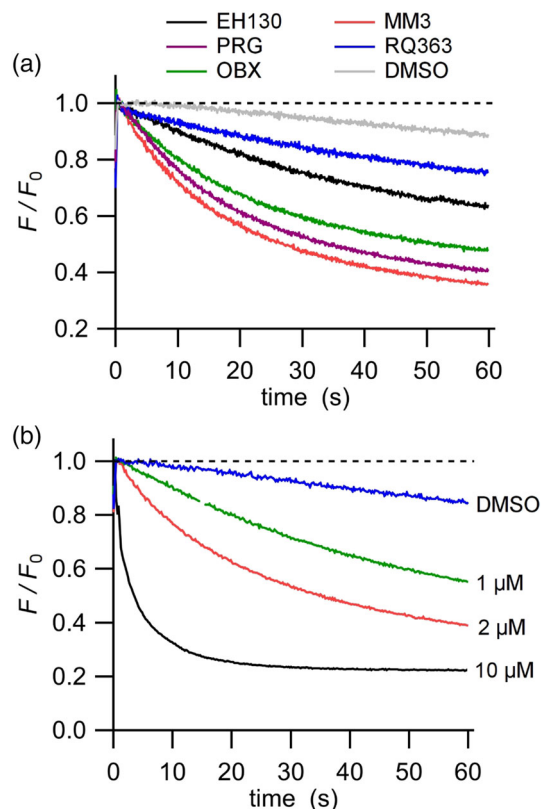
FIGURE 3 Iodide influx assay in FRT cells. The fluorescence is normalised to the initial value obtained after the addition of iodide. (a) YFP fluorescence decay by iodide influx upon addition of 2 μM of the different anionophores. Cells treated with DMSO were used as control. (b) The time course of the fluorescence decay in cells incubated at different concentrations of the anionophore MM3

FIGURE 4 The initial quenching rate (QR) of the YFP, indicating the iodide influx, is plotted against the concentration for the five studied compounds. Each point represents the means ± SEM from 6-10 determinations. The concentration–response curves, fitted with a Langmuir model (Equation 2), are represented as continuous lines. Fitting results are presented in Table 3

TABLE 3 Potency, as EC_{50}, and efficacy, as QR_{max}, of the anionophores tested on iodide transport in FRT cells

Compound	EC_{50} (μM)	QR_{max} ($1 \cdot \mu s^{-1}$)	PCC
EH130	2.2 ± 1.1	22.4 ± 1.1	0.904 (56)
Obatoclax	0.7 ± 0.1	32.7 ± 1.2	0.808 (64)
Prodigiosin	1.2 ± 0.1	63.0 ± 1.7	0.862 (63)
MM3	2.8 ± 0.6	334.9 ± 35.8	0.948 (49)
RQ363	2.4 ± 0.8	15.9 ± 1.4	0.860 (51)

The EC_{50} values represent the effective concentration to produce the half of the maximum transport, measured as the initial quenching rate. The QR_{max} values represent the maximum effect estimated from the fit of data presented in Figure 4 with Equation 2. PCC is the Pearson's correlation coefficient, and the number of data pairs is shown in parentheses.

with the anionophores (2 μM) caused a significant increase of the rate of iodide influx (Figure 3a). The QR was proportional to the concentration of the anionophore, as shown for MM3 in Figure 3b. For comparison, Figure S13 shows representative records obtained for all the anionophores studied, at two different concentrations.

Concentration–response curves for a given anionophore were constructed by plotting the average QR measured in six to 10 independent measurements at each concentration (Figure 4). The curves were well fitted with a first-order receptor-binding model (Kenakin, 2010)

$$QR(A) = QR_{max} \frac{A}{A + EC_{50}}, \qquad (2)$$

where A is the concentration of the anionophore, EC_{50} is effective concentration to produce the half of the maximum effect, QR_{max}. The fitting results are presented in Table 3. The relative potency of the anionophores measured in cells was different from that reported for LUV measurements. The EC_{50} of EH130 is not significantly different to those of the tambjamines MM3 and RQ363, and the most potent anionophores (with lower ED_{50}) are OBX and PRG. Instead, the efficacy of iodide transport, described by QR_{max}, shows that the tambjamine MM3 is the most effective transporter, being more than

fivefold more effective than the natural product PRG. The other two PRG-derived anionophores are less effective than PRG, yielding one half and one third QR_{max}, for OBX and EH130, respectively. The less effective anionophore is the second tambjamine studied, RQ363 (Figure 4 and Table 3). It is interesting to notice that the potency (EC_{50}) and the efficacy (QR_{max}) of these anionophores are not correlated, and therefore, both parameters need to be determined in choosing substances for an eventual therapeutic use.

3.5 | Effect of pH

We have previously reported that the transport efficacy of triazole derivatives of prodigiosin strongly depends on pH (Cossu et al., 2018; Hernando et al., 2018), which determines the ionisation state of these compounds (Cossu et al., 2018). Because all the anionophores studied have a protonable group involved in the chloride binding (Seganish & Davis, 2005; Díaz de Greñu et al., 2011; García-Valverde,

Alfonso, Quiñonero, & Quesada, 2012; Iglesias Hernández et al., 2012; Hernando, Soto-Cerrato, Cortés-Arroyo, Pérez-Tomás, & Quesada, 2014, 2018), with a pK_a plausibly near to the physiological pH, it is expected that the transport properties of all these substances will depend on the pH of the test system.

Thus, to confirm this hypothesis, we carried out transport assays with external solutions at pH 6.2 ($n = 6$ to 16), 6.6 ($n = 8$ to 57), 6.9 ($n = 6$ to 18), and 7.3 ($n = 11$ to 63) and found a significant increase of QR when the extracellular pH was set at acid values (Figure S14). Figure 5a–e shows how the mean QR, measured relative to the QR value at pH 7.3, varied with different pH. Notice that the reduction of 1.1 pH unit increased the activity of EH130 12-fold, OBX 9.3-fold, PRG 11.9-fold , MM3 2.8-fold , and RQ363 7.3-fold. The effects of acidification were more marked for prodigiosines than for the tambjamines (Figure 5f).
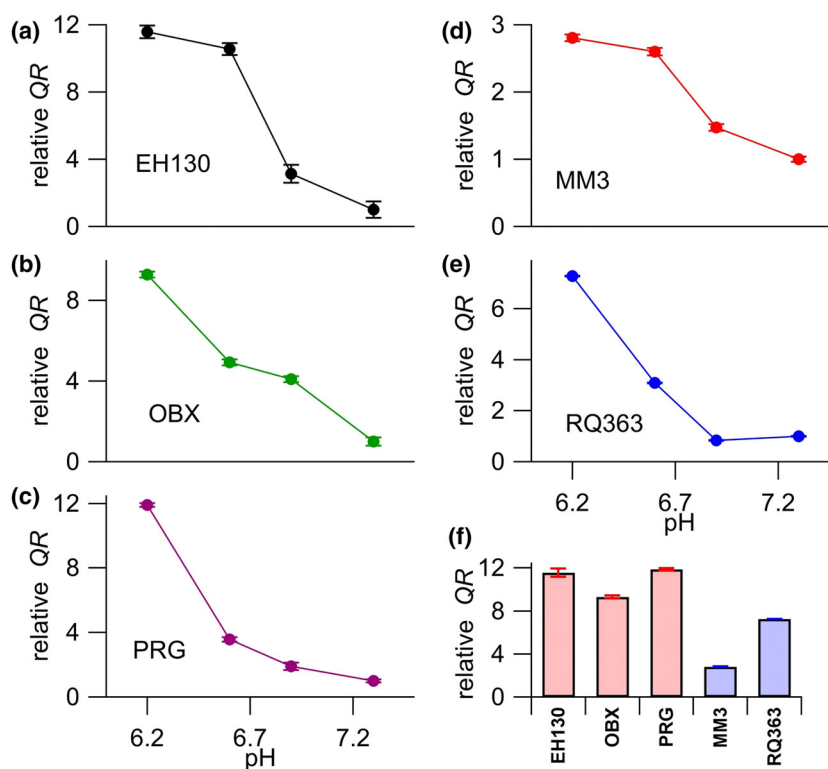
3.6 | Anion competition

To compare the chloride and iodide transport efficacy of anionophores, we substituted, iso-osmotically, the chloride in the extracellular solution by gluconate. Gluconate has a radius of 3.76 Å, which is significantly larger than the chloride radius of 1.81 Å (Schlumberger et al., 2014), and gluconate is not transported by triazole-derived prodigiosines in vesicles (Cossu et al., 2018). We hypothesised that chloride and iodide are competing for the same anion carriers and thus the substitution of chloride by gluconate will increase the iodide influx. Indeed, as expected, Figure 6a (red squares) shows that reduction of chloride results in an increase of the iodide influx driven by PRG. For

prodigiosines, statistical comparisons of the QR measured in the absence of chloride (51 mM gluconate) and in 51 mM chloride (0 gluconate) yield a significant increase of iodide transport by EH130, OBX and PRG (Figure 6b, red bars). Conversely, for the tambjamine MM3, the substitution of chloride by gluconate results in a reduction of iodide transport (Figure 6a, blue circles). In general, we observed a significant reduction of iodide transport in the tambjamines MM3 and RQ363 when chloride was substituted by gluconate (Figure 6b, blue bars). We hypothesise that, for the tambjamines, the increase of the gluconate concentration leads to the binding of this anion to the anionophore, forming a membrane impermeable complex and blocking iodide transport. By contrast, prodigiosines do not bind gluconate, and the reduction of the concentration of chloride results in more anion-free available transporters, and therefore favours the binding, and subsequent transport of iodide. Representative traces of these experiments are shown in Figure S15.

3.7 | Membrane potential

In the presence of extracellular chloride, the vehicle DMSO did not change the cell resting potential, as measured by the change in fluorescence ($\Delta F / F_0$) of the probe $DiBAC_4(3)$ (Figure 7). Incubation of cells with 2 μM of the prodigiosines (Figure 7) significantly decreased fluorescence, which is consistent with a hyperpolarisation of cells. A hyperpolarisation was also observed in the cells incubated with the tambjamine RQ363 (Figure 7). The extent of the hyperpolarisation is correlated with the efficacy of these anionophores (see Table 3).

FIGURE 5 The QR values, normalised to the value measured at pH 7.3, are plotted against the pH of the extracellular solution, for 2 μM of EH130 (a), OBX (b), PRG (c), MM3 (d), and RQ363 (e). The abscissa of panels (a) and (b) are the same as panel (c), and the abscissa of panel (d) is the same as that of panel (e). The number of measures for each anionophore at a given pH value was between six and 61. The normalised QR, showing the change produced by the reduction of pH from 7.3 to 6.2 is shown in (f). There, the bars representing prodigiosines are shown in red, and those for tambjamines are in blue
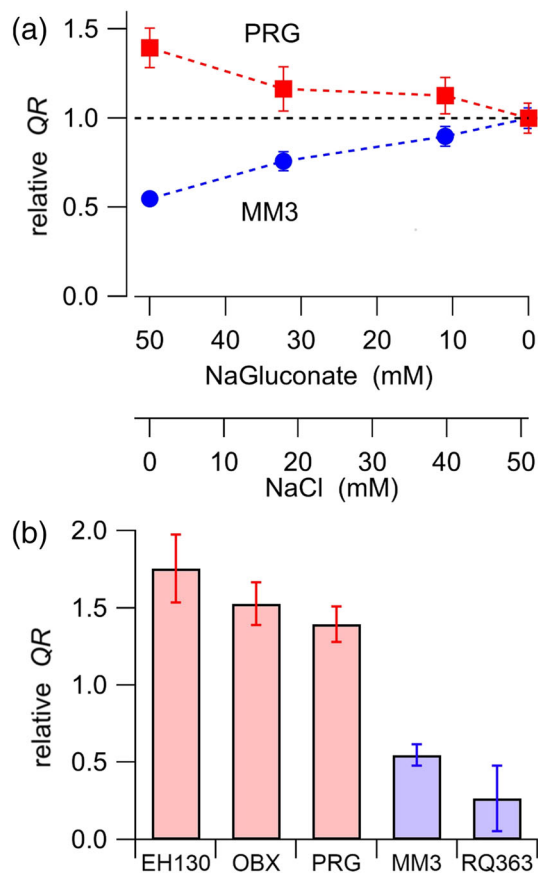
FIGURE 6 Effects of anion competition in iodide transport. (a) Iodide transport driven by PRG and MM3 were measured with different concentrations of chloride and gluconate in the extracellular solution. The relative QR represents the iodide influx measured at each combination of chloride and gluconate anions and was normalised to the QR measured with 51 mM chloride (0 gluconate). (b) Comparison of the iodide transport measured in gluconate and in chloride, expressed as the relative QR in the absence of chloride (and 51 mM gluconate) normalised by the QR measured at 51 mM chloride (and 0 gluconate). Red bars represent the prodigiosines and blue bars the tambjamines. Data are the means ± SEM from 6-13 measurements

However, the second tambjamine studied, MM3, did not induce any membrane potential change in the cells.

When the extracellular chloride is substituted by gluconate, the consequent intracellular chloride loss induced a cell hyperpolarisation, and the presence of the anionophores EH130, OBX, PRG, and RQ363 (Figure 7) did not further change significantly the cell membrane potential. Note that in the presence of gluconate, the anionophore MM3 did not change the membrane potential, relative to that of the untreated cells.

3.8 | Bicarbonate transport

The bicarbonate transport was studied with the NH_4^+ pulse protocol (Kintner et al., 2004) In this protocol, there is an intracellular acidification phase at the end of the NH_4^+ pulse, followed by an intracellular alkalinisation when NH_4^+ was removed and FRT cells were perfused
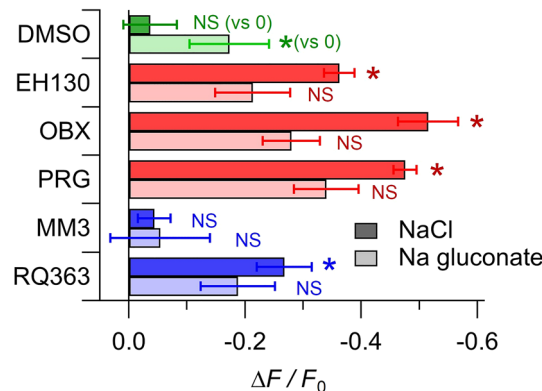

FIGURE 7 Relative change of the probe DiBAC4(3) fluorescence, normalised to the fluorescence of the untreated cells, measured in control cells treated with DMSO, and in cells incubated with 2 µM of different anionophores. Data shown are means ± SEM from at least 10 independent measurements. The DMSO controls were compared to the zero value; data from the cells treated with anionophores in the presence of chloride were compared with data from DMSO treated cells in the presence of chloride: data from the cells treated with anionophores in the presence of gluconate were compared with data from DMSO treated cells in the presence of gluconate. *$P < 0.05$, significantly different from corresponding DMSO value; NS, no significant difference; Student's t test

with bicarbonate (Figure 8a). This alkalinisation could be due to an influx of protons through the Na^+/H^+ exchange or to a bicarbonate influx through the Na^+/HCO_3^- co-transport and the Na^+-dependent and independent Cl^-/HCO_3^- exchangers. When the main bicarbonate and proton transport mechanisms were inhibited by 1 mM amiloride and 300 µM disodium-DIDS, respectively (Burnham, Amlal, Wang, Shull, & Soleimani, 1997; Lee et al., 1999; Shumaker & Soleimani, 1999), the extracellular bicarbonate does not enter the cell, leaving the pH_i constant (Figure 8b). Under these conditions, the perfusion of FRT cells with 2 µM EH130 (Figure 8c) or 2 µM MM3 (Figure 8d) results in a rapid increase of pH_i caused by the anionophore-induced bicarbonate influx. Observe that, in the absence of extracellular bicarbonate, application of the anionophore does not induce any pH_i change (Figure 8e). Similar experiments were carried out with FRT cells stably transfected with CFTR (FRT-CFTR cells) (Figure 8f). Also, in this case, the addition of 1 mM amiloride and 300 µM DIDS blocked the different bicarbonate pathways of the cells, and alkalinisation was observed only after the activation of CFTR by forskolin.

Application of 2 µM of EH130, OBX, PRG and MM3 changed the intracellular pH_i by an amount similar to that caused by the activation of the CFTR by 20 µM of forskolin (Figure 8g). A smaller, but still significant change of pH_i, was also caused by the tambjamine RQ363. In these experimental conditions, where cells are perfused with solutions equilibrated with 5% CO_2, and assuming that the CO_2 in extracellular space is in equilibrium with that of the intracellular space, it is possible to calculate the change in the intracellular concentration of bicarbonate applying the equation of Henderson–Hasselbach, as shown in the right axis in Figure 8g, indicating a net bicarbonate influx driven by the anionophores.

FIGURE 8 Intracellular pH measured during a NH$_4^+$ pulse protocol. Perfusion of FRT (a–e) and CFTR-FRT cells (f) with solutions saturated with 5% CO$_2$ are indicated at the top of the traces. (a) Perfusion with 40 mM NH$_4^+$ causes the alkalinisation of the cell, followed by a rapid acidification when external NH$_4^+$ is removed. Perfusion with bicarbonate immediately induced a pH$_i$ increase, correlated with the bicarbonate influx. (b) The main bicarbonate and proton transport mechanisms were inhibited by 1 mM amiloride and 300 μM DIDS and therefore, there is no pH$_i$ change. Perfusion with 2 μM EH130 (c) or 2 μM MM3 (d), in the presence of amiloride and DIDS, induced a pH$_i$ increase correlated with bicarbonate influx. (e) When anionophore is perfused in the absence of bicarbonate, there is no pH$_i$ change. (f) Similar experiments were performed on FRT–CFTR cells. Also, in this case, no pH$_i$ increase was observed until the activation of CFTR by forskolin (20 μM Fk). Each curve is the mean of at least four different regions in the acquired images. (g) The change of the pH$_i$, correlated with bicarbonate influx, upon perfusion of the cells with 2 μM of the prodigiosines EH130, OBX and PRG (red bars), the tambjamines MM3 and RQ363 (blue bars), and the activation of the CFTR by 20 μM forskolin. Data are the mean ± SEM of five independent experiments
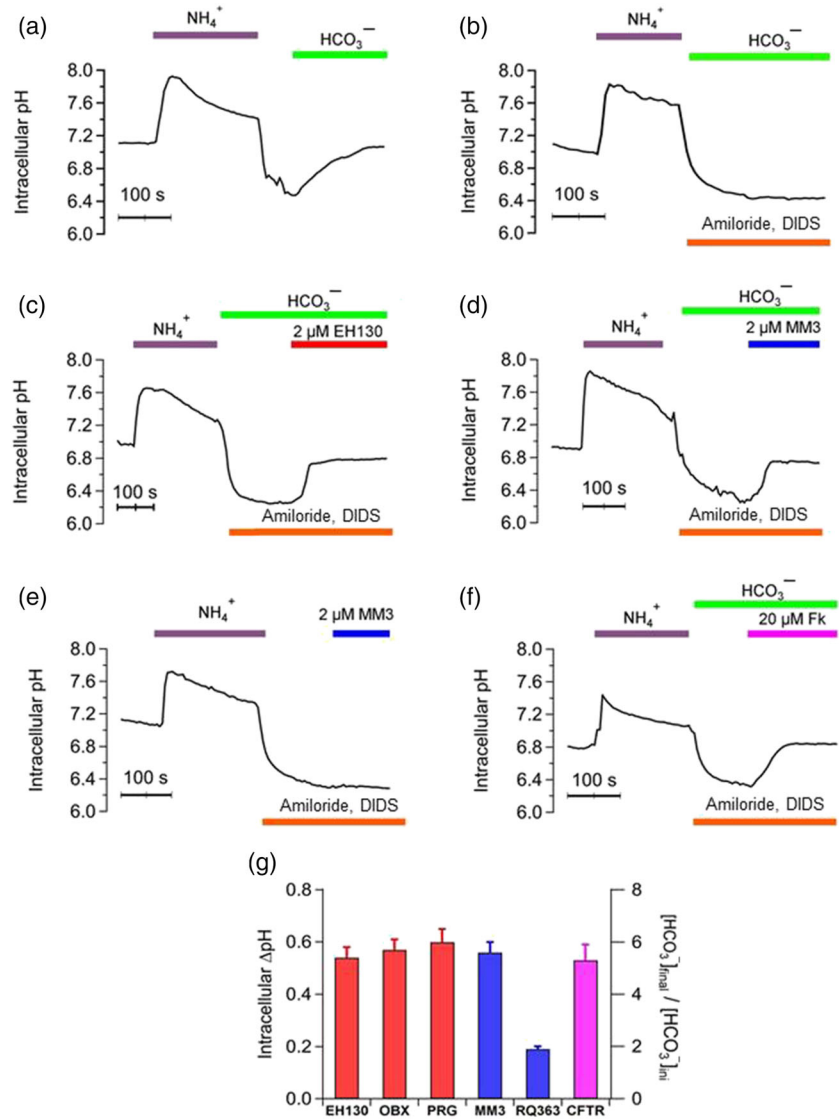
3.9 | Drug interaction

In control FRT cells transfected with CFTR, application of 20 μM forskolin elicits an iodide influx driven by the activation of the CFTR (Figure 9a). These cells expressing CFTR also show an iodide influx when treated with 2 μM anionophore, which is further increased when cells are treated with forskolin as well (Figure 9a). Notice that the anion influx in this group of experiments are roughly the sum of the transport due to the anionophore, represented by the light coloured bars in Figure 9a, and the transport driven by the CFTR shown as a magenta bar in Figure 9a. Moreover, a further increase of the CFTR-mediated anion transport occurs after the addition of the CFTR-potentiatior ivacaftor (10 μM; Figure 9a), also in the presence of anionophores. These data provide two important outcomes: The anionophores do not appear to acutely disrupt activation of CFTR by forskolin. The second result is that anionophores do not interfere with the mechanism of the CFTR potentiating drug, ivacaftor.

Similar experiments were carried out with FRT cells expressing the CF-mutant G551D (Figure 9b). In these cells, stimulation of CFTR by forskolin does not elicit any anion flux, as this mutation produces a gating defect on CFTR, reducing almost completely the capacity to open the channel. This defect was partly corrected using the potentiator ivacaftor (Figure 9b). Interestingly, an anion transport was also restored by treatment of the mutated-CFTR cells with anionophores (Figure 9b), but in this case, addition of forskolin did not further increase the anion transport, as the G551D-CFTR is not functional (Figure 9b). However, when the potentiator ivacaftor was added, there was a further increase of iodide influx, because of the addition of the anionophore-driven and the CFTR-mediated anion transport (Figure 9 b). Notice that the tambjamine MM3 is the most effective anion transporter in G551D-transfected cells.

The reduced anion transport in cells transfected with another mutant CFTR, F508del, can be efficiently restored by overnight treatment with the CFTR corrector lumacaftor (5 μM; Figure 9c).
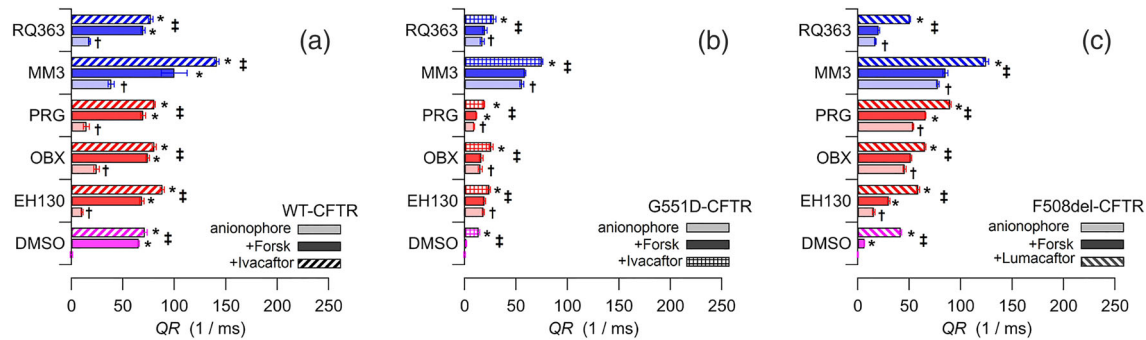
FIGURE 9 Iodide influx, expressed as the initial fluorescence quenching rate, QR, in FRT cells expressing WT-CFTR (a), G551D-CFTR (b), and F508del-CFTR (c). Magenta bars indicate the control experiments with the vehicle DMSO (and no anionophore); the red bars and the blue bars are experiments with 2 μM prodigiosines and tambjamines respectively. As shown in each panel, light colours indicate cells incubated with only the anionophore (or the vehicle), and the darker coloured bars correspond to cells treated with the anionophore plus 20 μM forskolin. WT-CFTR and G551D-CFTR cells treated with the anionophore, forskolin, and 10 μM ivacaftor are indicated by the striped bars in (a) and (b) respectively. Cells with the mutant F508del-CFTR pretreated with 5 μM lumacaftor overnight and incubated with the anionophore and forskolin are the striped bars in (c). Data are the mean ± SEM of 5–12 separate measurements. † $P < 0.05$, significantly different from control (vehicle DMSO); *$P < 0.05$, significant effect of forskolin; ‡ $P < 0.05$, significant effect of forskolin with ivacaftor or lumacaftor respectively; Student's t test

Application of anionophores produced a significant additional anion influx, which was further increased when CFTR was stimulated with forskolin (Figure 9c). The rescue of the F508del-CFTR is evident from the striped bars in Figure 9c, where cells were treated with lumacaftor and incubated with the anionophore and forskolin. These data confirm that, except for OBX, there is no interaction between the action of the anionophores and the corrective mechanism of lumacaftor. It is interesting to note that the efficacy of MM3 is the highest, and the increase of flux upon forskolin application is unexpectedly high.

4 | DISCUSSION

We have studied the anion transport properties of a set of synthetic compounds, named anionophores. These substances belong to two chemical families: the prodigiosines (PRG, OBX and EH130) and the tambjamines (MM3 and RQ363). The two groups have a very similar structural motif, with three NH groups, one of them ionisable with a pK$_a$ between 6 and 7 (see Figure S1). The difference between the two groups is that the ionisable NH group in the tambjamines is an imine, and in the prodigiosines is located in an azafulvene heterocycle. Solid state X-ray diffraction studies, ab initio theoretical calculations, and NMR analysis of these compounds have demonstrated that all these molecules can coordinate an anion through hydrogen bonds to the three NH groups (Díaz de Greñu et al., 2011; García-Valverde, Alfonso, Quiñonero, & Quesada, 2012; Hernando et al., 2018; Hernando, Soto-Cerrato, Cortés-Arroyo, Pérez-Tomás, & Quesada, 2014; Iglesias Hernández et al., 2012; Soto-Cerrato et al., 2015). As reported elsewhere (Cossu et al., 2018; Díaz de Greñu et al., 2011; Hernando et al., 2018; Hernando, Soto-Cerrato, Cortés-Arroyo, Pérez-Tomás, & Quesada, 2014; Iglesias Hernández et al., 2012; Saggiomo et al., 2012), EH130, PRG, OBX, and RQ363 can exchange chloride for nitrate across the bilayer membrane in a vesicle model

(see also Figure S7–S11). Here, we report that the tambjamine MM3 also has similar anion transporting properties (Figure 1b,c).

To use these substances in cells, as possible therapeutic drugs, is a big challenge, as these molecules are derivatives of cytotoxic natural products. Indeed, compounds like OBX have been proposed as antitumor chemotherapeutic agents (Hernando, Soto-Cerrato, Cortés-Arroyo, Pérez-Tomás, & Quesada, 2014; Ko et al., 2014; Rodilla et al., 2017). An effort to reduce the toxicity of the PRG-related compounds has been successful by preparing the triazole derivatives of PRG (Cossu et al., 2018; Hernando et al., 2018). Now, we also have used two tambjamines, MM3 and RQ363, which are clearly less toxic than the prodigiosines (Table 2), to analyse their anion transporting properties in cells. To our knowledge, this is the first report of tambjamine-driven anion transport in living mammalian cells. These data are compared with the results obtained with prodigiosines to have a better insight on the anion transport mechanisms by these two families of anionophores.

The first experiments were to reproduce in cells, the chloride efflux measurements already well established in unilamellar vesicles. However, although it was possible to record anionophore-driven chloride effluxes (Figure 2), quantification of these effects was made difficult by several technical problems. First, because the intracellular chloride concentration in epithelial cells is low, between 20 and 40 mM (Bregestovski, Waseem, & Mukhtarov, 2009; Falkenberg & Jakobsson, 2010; Treharne, Crawford, & Mehta, 2006; Willumsen, Davis, & Boucher, 1989), even when the extracellular chloride concentrations were reduced close to zero, the concentration gradient was still very small, and the magnitude of the efflux was consequently reduced. These conditions also influence the resolution of the measurements, as the chloride leaving the cell is further diluted in the external solution, reaching extracellular chloride concentrations at the limit of the ion-sensitive electrodes. On the other hand, keeping the cells in a low chloride solution, even for short periods of time, induces an

intracellular chloride depletion, further reducing the chloride gradient, and causes the activation of the cell mechanisms aimed at normalising the ion concentrations, which in turn may interfere with our measurements of anionophore transport. Thus, we continued the analysis using the iodide influx, by measuring the kinetics of the fluorescence quenching of iodide-sensitive YFP. This method, originally developed to perform high-throughput screening for searching substances that could potentiate or correct the mutant CFTR, is quite well standardised (Galietta, Haggie, & Verkman, 2001; Galietta, Jayaraman, & Verkman, 2001). The method has the advantage that, assuming that initially there is no iodide in the intracellular space, the iodide injection at the beginning of the assay provides a constant iodide gradient, and therefore, the initial quenching rate will be directly proportional to the iodide permeability. Thus, we could measure the anion influx driven by different anionophores by analysing the fluorescence quenching curves (Figure 3a) and study the concentration dependence of the transport activity of different anionophores (Figure 3b). With this procedure, we constructed the concentration–response curves for all the studied anionophores (Figure 4) and fit them with a first-order ligand–receptor model that yields the potency of the anionophores, in terms of EC_{50}, and the efficacy, expressed as the maximum quenching rate, QR_{max} (Table 3).

Chloride transport in mammalian cells was further assessed by the measurement of the relative membrane potential using fluorescence probes (Figure 7). When an anionophore is applied, it leads to a hyperpolarisation of the cell, consistent with a chloride influx. Substituting the extracellular chloride by gluconate induces a hyperpolarisation, and probably a loss of chloride from the cell with no further changes in membrane potential when anionophores are added. Surprisingly, the effects on membrane potential of the tambjamine MM3 were completely different. This anionophore did not cause any membrane potential changes, even though it was the most effective transporter of the studied series, and further studies are needed to more thoroughly investigate this observation.

Bicarbonate transport is a mandatory attribute to include when designing a compound as substitution treatments for CF. Indeed, in CF subjects and animal models, there is a significantly reduced bicarbonate concentration, as well as lower pH, in the airway surface liquid (Abou Alaiwa et al., 2014; Ostedgaard et al., 2011; Pezzulo et al., 2012; Quinton, 1999, 2008). This situation compromises the post-secretory MUC5AC and MUC5B processes, resulting in an increased mucus viscosity (Abdullah et al., 2017; Quinton, 2008; Tang et al., 2016). We have assessed the transport of bicarbonate, as changes in pH_i in conditions of controlled CO_2 and suppression of the most important endogenous cellular bicarbonate and proton transporters. Our data show that all the anionophores tested were able to transport bicarbonate into cells, restoring the intracellular bicarbonate to the same values as those obtained by the stimulation of CFTR, except for RQ363, that has a lower bicarbonate transport capability.

The transport activity of these anionophores increases as the pH become more acid (Figure 5). This effect is due to the presence of an ionisable group in the molecule, as these anionophores are active in their protonated form (Cossu et al., 2018). This sensitivity is more prominent for the prodigiosines than the tambjamines (Figure 5f), as the main difference between these two anionophore families is the type of ionisable NH (an azafulvene in the prodigiosines and an imine in the tambjamines). However, it can also be ascribed to a putative structural difference in the structure of their anion binding site. This difference in the anion binding site was further revealed in the anion substitution experiments (Figure 6). When measuring the iodide influx in the prodigiosines, the substitution of extracellular chloride with gluconate increased iodide transport up to 1.5-fold. This is probably because, as gluconate does not bind to the prodigiosines, the chloride and iodide anions compete for the binding site of the anionophore, and substitution of chloride by gluconate leaves more molecules free to transport iodide. By contrast, tambjamine-driven iodide influx was reduced by about half, when chloride is substituted by gluconate. This paradoxical difference can be justified if gluconate is able to bind the tambjamine binding site, perhaps more tightly than chloride, and competing with iodide for the anionophores, decreasing the availability of tambjamines to bind iodide, and consequently reducing the flux. These data clearly demonstrate that the interaction of various anions with the prodigiosines and the tambjamines is different, perhaps indicating differences in the fine structure of the anion binding site.

The estimated anion transport carried by the CFTR, expressed as the QR measured after stimulation of the WT-CFTR with 20 μM forskolin, was 65.1 ms^{-1} (Figure 9a). However, it should be noted that the activity of the WT-CFTR measured as short-circuit current on FRT epithelia stably transfected with CFTR is much higher (10.6 times) than CFTR endogenously expressed in primary human bronchial epithelia (Pedemonte, Tomati, Sondo, & Galietta, 2010). Thus, a heuristic goal for the anionophores would be to achieve a transport equivalent to a QR of 6.3 ms^{-1}. The concentration of anionophores to produce this transport rate calculated from the data on Table 3 is, in most cases, below micromolar concentration (0.86, 0.17, 0.13, 0.054, and 1.65 μM for EH130, OBX, PRG, MM3, and RQ363, respectively). Note that these concentrations are, at least, one order of magnitude below the TD_{50} measured for the three cell lines (see Table 2). To further restrict the toxic effects of these anionophores, we compared the concentration needed to obtain the target QR of 6.3 ms^{-1} with the anionophore concentration for 99% of cell survival, TD_1. None of the PRGs conform to this additional restriction, as the TD_1 for EH130, OBX, and PRG are 9.5, 4, and 3.4 times higher than the concentration for the target QR. Because of its low efficacy, the concentration of the tambjamine RQ363 for the target QR is 7.4 times the TD_1. Conversely, the high efficacy of the tambjamine MM3 results in a very low concentration for the target QR, which was 0.24 of the TD_1.

Finally, we assessed the possibility of interference between the anionophores and the activation of the CFTR by forskolin, or between the anionophores and the clinically used CFTR potentiator ivacaftor and the CFTR-corrector lumacaftor. Measurements in cells expressing WT-CFTR showed that the iodide influx promoted by the anionophores was more or less additive to that driven by the CFTR

(Figure 9a). Addition of ivacaftor increased the CFTR activity further, indicating that these anionophores did not interfere with the CFTR potentiator's action. This important fact is confirmed by the results obtained in FRT cells expressing G551D-CFTR (Figure 9b), where the anion transport resulting from rescue of the mutated-CFTR activity by ivacaftor was additive to that driven by the anionophores. Similar results were also obtained in the mutant F508del (Figure 9c). The minimal level of anion transport, resulting from the severely reduced F508del-CFTR activity, was still increased by the anionophore-driven transport. When the F508del-CFTR was rescued by the corrector lumacaftor, the restored CFTR activity was added to that of the anionophores.

These experiments demonstrated that these anionophores could be used to promote chloride and bicarbonate transport in cells. They are, therefore, good candidates to replace the defective or missing CFTR, in an attempt to design a new CF therapy, as proposed for other anion transporters (Dias et al., 2018; Li et al., 2016; Liu et al., 2016; Shen, Li, Wang, Yao, & Yang, 2012; Valkenier et al., 2014). The analysis of anionophore-induced anion transport in cells needs, in any case, to be extended, exploring the effects of long-term treatment with anionophores in cells, and studying anionophore-induced ion transport in epithelial models, where the polarisation of cells plays a crucial role in the direction of ion transport, in order to find the compounds best suited to become candidates for CF therapy.

In conclusion, we have shown that the two types of anionophore studied here were able to transport halides and bicarbonate in mammalian cells, with an efficiency similar to that of the native CFTR, opening the way to a treatment for CF based on a substitutive transport mechanism. The transport efficacy of these anionophores is high enough to allow their use at concentrations significantly lower than their cytotoxic concentrations. Perhaps the two PRGs, PRG and OBX, which have been described also as apoptosis promoters (Díaz de Greñu et al., 2011; Hosseini et al., 2013), are not appropriate for continuing these studies, but the others, in particular MM3, are very good candidates for further analysis and for the improvement of the properties of the molecule. The definite proof of concept to drive the research for better, less toxic and more efficient compounds will come from further studies in a complex cellular system, such as bronchial and epithelial models, where the cell polarisation defines more precisely the transport characteristics of the cells, closer to the physiological and pathophysiological systems. Overall, these results represent an encouraging approach to the development of a mutant-independent CF therapy.

ACKNOWLEDGEMENT

AUTHOR CONTRIBUTIONS

O.M. and M.F. designed the experiments. R.Q., M.M., and I.C.-B. synthesised the compounds. M.F., R.Q., M.M., I.C.-B., A.L., V.C., C.P., E.C., and D.B. performed the experiments and data analysis. O.M. wrote the manuscript. O.M., R.Q., and E.C. have full access to all the data in the study and take responsibility for the integrity of the data and the accuracy of the data analysis.

CONFLICT OF INTEREST

The authors declare no conflicts of interest.

DECLARATION OF TRANSPARENCY AND SCIENTIFIC RIGOUR

This Declaration acknowledges that this paper adheres to the principles for transparent reporting and scientific rigour of preclinical research as stated in the *BJP* guidelines for Design & Analysis, and as recommended by funding agencies, publishers and other organisations engaged with supporting research.

ORCID

Oscar Moran https://orcid.org/0000-0003-1287-6176

REFERENCES

Abdullah, L. H., Evans, J. R., Wang, T. T., Ford, A. A., Makhov, A. M., Nguyen, K., ... Kesimer, M. (2017). Defective postsecretory maturation of MUC5B mucin in cystic fibrosis airways. *JCI Insight*, *2*, e89752.

Abou Alaiwa, M. H., Beer, A. M., Pezzulo, A. A., Launspach, J. L., Horan, R. A., Stoltz, D. A., ... Zabner, J. (2014). Neonates with cystic fibrosis have a reduced nasal liquid pH: A small pilot study. *Journal of Cystic Fibrosis*, *13*, 373–377. https://doi.org/10.1016/j.jcf.2013.12.006

Alexander, S. P. H., Kelly, E., Marrion, N. V., Peters, J. A., Faccenda, E., Harding, S. D., ... CGTP Collaborators (2017). The Concise Guide to PHARMACOLOGY 2017/18: Other ion channels. *British Journal of Pharmacology*, *174*, S195–S207. https://doi.org/10.1111/bph.13881

Black, J. W., & Leff, P. (1983). Operational models of pharmacological agonism. *Proceedings of the Royal Society of London - Series B: Biological Sciences*, *220*, 141–162.

Bobadilla, J. L., Macek, M. J., Fine, J. P., & Farrell, P. M. (2002). Cystic fibrosis: A worldwide analysis of CFTR mutations-correlation with incidence data and application to screening. *Human Mutation*, *19*, 575–606. https://doi.org/10.1002/humu.10041

Boyle, M. P., Bell, S. C., Konstan, M. W., McColley, S. A., Rowe, S. M., Rietschel, E., ... VX09-809-102 study group (2014). A CFTR corrector (lumacaftor) and a CFTR potentiator (ivacaftor) for treatment of patients with cystic fibrosis who have a phe508del CFTR mutation: A phase 2 randomised controlled trial. *The Lancet Respiratory Medicine*, *2*, 527–538. https://doi.org/10.1016/S2213-2600(14)70132-8

Bregestovski, P., Waseem, T., & Mukhtarov, M. (2009). Genetically encoded optical sensors for monitoring of intracellular chloride and chloride-selective channel activity. *Frontiers in Molecular Neuroscience*, *2*, 15.

Burnham, C. E., Amlal, H., Wang, Z., Shull, G. E., & Soleimani, M. (1997). Cloning and functional expression of a human kidney Na+: HCO3− cotransporter. *The Journal of Biological Chemistry*, *272*, 19111–19114. https://doi.org/10.1074/jbc.272.31.19111

Caci, E., Caputo, A., Hinzpeter, A., Arous, N., Fanen, P., Sonawane, N., ... Galietta, L. J. V. (2008). Evidence for direct CFTR inhibition by CFTR (inh)-172 based on Arg347 mutagenesis. *The Biochemical Journal*, *413*, 135–142. https://doi.org/10.1042/BJ20080029

Castellani, C., & Assael, B. M. (2017). Cystic fibrosis: A clinical view. *Cellular and Molecular Life Sciences*, *74*, 129–140. https://doi.org/10.1007/s00018-016-2393-9

Clancy, J. P., Rowe, S. M., Accurso, F. J., Aitken, M. L., Amin, R. S., Ashlock, M. A., ... Konstan, M. W. (2012). Results of a phase IIa study of VX-809, an investigational CFTR corrector compound, in subjects with cystic fibrosis homozygous for the F508del-CFTR mutation. *Thorax*, *67*, 12–18. https://doi.org/10.1136/thoraxjnl-2011-200393

Cossu, C., Fiore, M., Baroni, D., Capurro, V., Caci, E., Garcia Valverde, M., ... Moran, O. (2018). Anion-transport mechanism of a triazole-bearing derivative of prodigiosine: A candidate for cystic fibrosis therapy. *Frontiers in Pharmacology*, *9*. https://doi.org/10.3389/fphar.2018.00852

Curtis, M. J., Alexander, S., Cirino, G., Docherty, J. R., George, C. H., Giembycz, M. A., ... Ahluwalia, A. (2018). Experimental design and analysis and their reporting II: updated and simplified guidance for authors and peer reviewers. *British Journal of Pharmacology*, *175*, 987–993. https://doi.org/10.1111/bph.14153

Davies, J. C., Moskowitz, S. M., Brown, C., Horsley, A., Mall, M. A., McKone, E. F., ... VX16-659-101 Study Group (2018). VX-659–tezacaftor–ivacaftor in patients with cystic fibrosis and one or two Phe508del alleles. *The New England Journal of Medicine*, *379*, 1599–1611. https://doi.org/10.1056/NEJMoa1807119

Davis, J. T., Okunola, O., & Quesada, R. (2010). Recent advances in the transmembrane transport of anions. *Chemical Society Reviews*, *39*, 3843–3862. https://doi.org/10.1039/b926164h

De Boeck, K., & Davies, J. C. (2017). Where are we with transformational therapies for patients with cystic fibrosis? *Current Opinion in Pharmacology*, *34*, 70–75. https://doi.org/10.1016/j.coph.2017.09.005

Dias, C. M., Li, H., Valkenier, H., Karagiannidis, L. E., Gale, P. A., Sheppard, D. N., & Davis, A. P. (2018). Anion transport by ortho-phenylene bis-ureas across cell and vesicle membranes. *Organic & Biomolecular Chemistry*, *16*, 1083–1087. https://doi.org/10.1039/C7OB02787G

Díaz de Greñu, B., Iglesias Hernández, P., Espona, M., Quiñonero, D., Light, M. E., Torroba, T., ... Quesada, R. (2011). Synthetic prodiginine obatoclax (GX15-070) and related analogues: Anion binding, transmembrane transport, and cytotoxicity properties. *Chemistry*, *17*, 14074–14083. https://doi.org/10.1002/chem.201101547

Eckford, P. D. W., Li, C., Ramjeesingh, M., & Bear, C. E. (2012). Cystic fibrosis transmembrane conductance regulator (CFTR) potentiator VX-770 (ivacaftor) opens the defective channel gate of mutant CFTR in a phosphorylation-dependent but ATP-independent manner. *The Journal of Biological Chemistry*, *287*, 36639–36649. https://doi.org/10.1074/jbc.M112.393637

Falkenberg, C. V., & Jakobsson, E. (2010). A biophysical model for integration of electrical, osmotic, and pH regulation in the human bronchial epithelium. *Biophysical Journal*, *98*, 1476–1485. https://doi.org/10.1016/j.bpj.2009.11.045

Galietta, L., Haggie, P., & Verkman, A. (2001). Green fluorescent protein-based halide indicators with improved chloride and iodide affinities. *FEBS Letters*, *499*, 220–224. https://doi.org/10.1016/S0014-5793(01)02561-3

Galietta, L. J. V. (2013). Managing the underlying cause of cystic fibrosis: A future role for potentiators and correctors. *Paediatric Drugs*, *15*, 393–402. https://doi.org/10.1007/s40272-013-0035-3

Galietta, L. V., Jayaraman, S., & Verkman, A. S. (2001). Cell-based assay for high-throughput quantitative screening of CFTR chloride transport agonists. *American Journal of Physiology. Cell Physiology*, *281*, C1734–C1742. https://doi.org/10.1152/ajpcell.2001.281.5.C1734

García-Valverde, M., Alfonso, I., Quiñonero, D., & Quesada, R. (2012). Conformational analysis of a model synthetic prodiginine. *The Journal of Organic Chemistry*, *77*, 6538–6544. https://doi.org/10.1021/jo301008c

Gianotti, A., Melani, R., Caci, E., Sondo, E., Ravazzolo, R., Galietta, L. J. V., & Zegarra-Moran, O. (2013). Epithelial sodium channel silencing as a strategy to correct the airway surface fluid deficit in cystic fibrosis. *American Journal of Respiratory Cell and Molecular Biology*, *49*, 445–452. https://doi.org/10.1165/rcmb.2012-0408OC

Hadida, S., Van Goor, F., Zhou, J., Arumugam, V., McCartney, J., Hazlewood, A., ... Grootenhuis, P. D. (2014). Discovery of N-(2,4-di-tert-butyl-5-hydroxyphenyl)-4-oxo-1,4-dihydroquinoline-3-carboxamide (VX-770, ivacaftor), a potent and orally bioavailable CFTR potentiator. *Journal of Medicinal Chemistry*, *57*, 9776–9795. https://doi.org/10.1021/jm5012808

Harding, S. D., Sharman, J. L., Faccenda, E., Southan, C., Pawson, A. J., Ireland, S., ... NC-IUPHAR (2018). The IUPHAR/BPS guide to pharmacology in 2018: Updates and expansion to encompass the new guide to immunopharmacology. *Nucleic Acids Research*, *46*, D1091–D1106. https://doi.org/10.1093/nar/gkx1121

Hartzell, C., Putzier, I., & Arreola, J. (2005). Calcium-activated chloride channels. *Annual Review of Physiology*, *67*, 719–758. https://doi.org/10.1146/annurev.physiol.67.032003.154341

Hernando, E., Capurro, V., Cossu, C., Fiore, M., García-Valverde, M., Soto-Cerrato, V., ... Quesada, R. (2018). Small molecule anionophores promote transmembrane anion permeation matching CFTR activity. *Scientific Reports*, *8*, 2608. https://doi.org/10.1038/s41598-018-20708-3

Hernando, E., Soto-Cerrato, V., Cortés-Arroyo, S., Pérez-Tomás, R., & Quesada, R. (2014). Transmembrane anion transport and cytotoxicity of synthetic tambjamine analogs. *Organic & Biomolecular Chemistry*, *12*, 1771–1778. https://doi.org/10.1039/C3OB42341G

Hosseini, A., Espona-Fiedler, M., Soto-Cerrato, V., Quesada, R., Pérez-Tomás, R., & Guallar, V. (2013). Molecular interactions of prodiginines with the BH3 domain of anti-apoptotic Bcl-2 family members. *PLoS ONE*, *8*, e57562. https://doi.org/10.1371/journal.pone.0057562

Hudock, K. M., & Clancy, J. P. (2017). An update on new and emerging therapies for cystic fibrosis. *Expert Opinion on Emerging Drugs*, *22*, 331–346. https://doi.org/10.1080/14728214.2017.1418324

Iglesias Hernández, P., Moreno, D., Javier, A. A., Torroba, T., Pérez-Tomás, R., & Quesada, R. (2012). Tambjamine alkaloids and related synthetic analogs: Efficient transmembrane anion transporters. *Chemical Communications(Camb.)*, *48*, 1556–1558. https://doi.org/10.1039/C1CC11300C

Kenakin, T. P. (2010). *A pharmacology primer: Theory, applications, and methods*, Amsterdam, Elsevier/Academic press.

Kintner, D. B., Su, G., Lenart, B., Ballard, A. J., Meyer, J. W., Ng, L. L., ... Sun, D. (2004). Increased tolerance to oxygen and glucose deprivation in astrocytes from Na^+/H^+ exchanger isoform 1 null mice. *American Journal of Physiology. Cell Physiology*, *287*, C12–C21. https://doi.org/10.1152/ajpcell.00560.2003

Ko, S.-K., Kim, S. K., Share, A., Lynch, V. M., Park, J., Namkung, W., ... Shin, I. (2014). Synthetic ion transporters can induce apoptosis by facilitating chloride anion transport into cells. *Nature Chemistry*, *6*, 885–892. https://doi.org/10.1038/nchem.2021

Lee, M. G., Wigley, W. C., Zeng, W., Noel, L. E., Marino, C. R., Thomas, P. J., & Muallem, S. (1999). Regulation of $Cl^-/HCO3^-$ exchange by cystic fibrosis transmembrane conductance regulator expressed in NIH 3T3 and HEK 293 cells. *The Journal of Biological Chemistry*, *274*, 3414–3421. https://doi.org/10.1074/jbc.274.6.3414

Li, H., Salomon, J. J., Sheppard, D. N., Mall, M. A., & Galietta, L. J. (2017). Bypassing CFTR dysfunction in cystic fibrosis with alternative

pathways for anion transport. *Current Opinion in Pharmacology*, *34*, 91–97. https://doi.org/10.1016/j.coph.2017.10.002

Li, H., Valkenier, H., Judd, L. W., Brotherhood, P. R., Hussain, S., Cooper, J. A., ... Davis, A. P. (2016). Efficient, non-toxic anion transport by synthetic carriers in cells and epithelia. *Nature Chemistry*, *8*, 24–32. https://doi.org/10.1038/nchem.2384

Liu, P.-Y., Li, S.-T., Shen, F.-F., Ko, W.-H., Yao, X.-Q., & Yang, D. (2016). A small synthetic molecule functions as a chloride-bicarbonate dual-transporter and induces chloride secretion in cells. *Chemical Communications(Camb.)*, *52*, 7380–7383. https://doi.org/10.1039/C6CC01964A

Loo, T. W., & Clarke, D. M. (2017). Corrector VX-809 promotes interactions between cytoplasmic loop one and the first nucleotide-binding domain of CFTR. *Biochemical Pharmacology*, *136*, 24–31. https://doi.org/10.1016/j.bcp.2017.03.020

Louis, K. S., & Siegel, A. C. (2011). Cell viability analysis using trypan blue: Manual and automated methods. *Methods in Molecular Biology*, *740*, 7–12. https://doi.org/10.1007/978-1-61779-108-6_2

Ostedgaard, L. S., Meyerholz, D. K., Chen, J.-H., Pezzulo, A. A., Karp, P. H., Rokhlina, T., ... Stoltz, D. A. (2011). The ΔF508 mutation causes CFTR misprocessing and cystic fibrosis-like disease in pigs. *Science Translational Medicine*, *3*, 74ra24.

Pedemonte, N., Tomati, V., Sondo, E., & Galietta, L. J. V. (2010). Influence of cell background on pharmacological rescue of mutant CFTR. *American Journal of Physiology. Cell Physiology*, *298*, C866–C874. https://doi.org/10.1152/ajpcell.00404.2009

Pezzulo, A. A., Tang, X. X., Hoegger, M. J., Abou Alaiwa, M. H., Ramachandran, S., Moninger, T. O., ... Zabner, J. (2012). Reduced airway surface pH impairs bacterial killing in the porcine cystic fibrosis lung. *Nature*, *487*, 109–113. https://doi.org/10.1038/nature11130

Quinton, P. M. (1999). Physiological basis of cystic fibrosis: A historical perspective. *Physiological Reviews*, *79*, S3–S22. https://doi.org/10.1152/physrev.1999.79.1.S3

Quinton, P. M. (2008). Cystic fibrosis: Impaired bicarbonate secretion and mucoviscidosis. *Lancet*, *372*, 415–417. https://doi.org/10.1016/S0140-6736(08)61162-9

Ramsey, B. W., Davies, J., McElvaney, N. G., Tullis, E., Bell, S. C., Dřevínek, P., et al. (2011). A CFTR potentiator in patients with cystic fibrosis and the G551D mutation. *The New England Journal of Medicine*, *365*, 1663–1672. https://doi.org/10.1056/NEJMoa1105185

Rapoport, H., & Holden, K. G. (1962). The synthesis of prodigiosin. *Journal of the American Chemical Society*, *84*, 635–642. https://doi.org/10.1021/ja00863a026

Ren, H. Y., Grove, D. E., De La Rosa, O., Houck, S. A., Sopha, P., Van Goor, F., ... Cyr, D. M. (2013). VX-809 corrects folding defects in cystic fibrosis transmembrane conductance regulator protein through action on membrane-spanning domain 1. *Molecular Biology of the Cell*, *24*, 3016–3024. https://doi.org/10.1091/mbc.e13-05-0240

Rodilla, A. M., Korrodi-Gregório, L., Hernando, E., Manuel-Manresa, P., Quesada, R., Pérez-Tomás, R., & Soto-Cerrato, V. (2017). Synthetic tambjamine analogues induce mitochondrial swelling and lysosomal dysfunction leading to autophagy blockade and necrotic cell death in lung cancer. *Biochemical Pharmacology*, *126*, 23–33. https://doi.org/10.1016/j.bcp.2016.11.022

Saggiomo, V., Otto, S., Marques, I., Félix, V., Torroba, T., & Quesada, R. (2012). The role of lipophilicity in transmembrane anion transport. *Chemical Communications(Camb.)*, *48*, 5274–5276. https://doi.org/10.1039/c2cc31825c

Schlumberger, S., Kristan, K. Č., Ota, K., Frangež, R., Molgó, J., Sepčić, K., ... Maček, P. (2014). Permeability characteristics of cell-membrane pores induced by ostreolysin A/pleurotolysin B, binary pore-forming proteins

from the oyster mushroom. *FEBS Letters*, *588*, 35–40. https://doi.org/10.1016/j.febslet.2013.10.038

Seganish, J. L., & Davis, J. T. (2005). Prodigiosin is a chloride carrier that can function as an anion exchanger. *Chemical Communications(Camb.)*, *46*, 5781–5783. https://doi.org/10.1039/b511847f

Shen, B., Li, X., Wang, F., Yao, X., & Yang, D. (2012). A synthetic chloride channel restores chloride conductance in human cystic fibrosis epithelial cells. *PLoS ONE*, *7*, e34694. https://doi.org/10.1371/journal.pone.0034694

Shumaker, H., & Soleimani, M. (1999). CFTR upregulates the expression of the basolateral Na^+-K^+-$2Cl^-$ cotransporter in cultured pancreatic duct cells. *The American Journal of Physiology*, *277*, C1100–C1110. https://doi.org/10.1152/ajpcell.1999.277.6.C1100

Soto-Cerrato, V., Manuel-Manresa, P., Hernando, E., Calabuig-Fariñas, S., Martínez-Romero, A., Fernández-Dueñas, V., ... Quesada, R. (2015). Facilitated anion transport induces hyperpolarization of the cell membrane that triggers differentiation and cell death in cancer stem cells. *Journal of the American Chemical Society*, *137*, 15892–15898. https://doi.org/10.1021/jacs.5b09970

Strausbaugh, S. D., & Davis, P. B. (2007). Cystic fibrosis: A review of epidemiology and pathobiology. *Clinics in Chest Medicine*, *28*, 279–288. https://doi.org/10.1016/j.ccm.2007.02.011

Tang, X. X., Ostedgaard, L. S., Hoegger, M. J., Moninger, T. O., Karp, P. H., McMenimen, J. D., ... Welsh, M. J. (2016). Acidic pH increases airway surface liquid viscosity in cystic fibrosis. *The Journal of Clinical Investigation*, *126*, 879–891. https://doi.org/10.1172/JCI83922

Treharne, K. J., Crawford, R. M., & Mehta, A. (2006). CFTR, chloride concentration and cell volume: Could mammalian protein histidine phosphorylation play a latent role? *Experimental Physiology*, *91*, 131–139. https://doi.org/10.1113/expphysiol.2005.031823

Valkenier, H., Judd, L. W., Li, H., Hussain, S., Sheppard, D. N., & Davis, A. P. (2014). Preorganized bis-thioureas as powerful anion carriers: Chloride transport by single molecules in large unilamellar vesicles. *Journal of the American Chemical Society*, *136*, 12507–12512. https://doi.org/10.1021/ja507551z

Van Goor, F., Hadida, S., Grootenhuis, P. D. J., Burton, B., Stack, J. H., Straley, K. S., ... Negulescu, P. A. (2011). Correction of the F508del-CFTR protein processing defect in vitro by the investigational drug VX-809. *Proceedings of the National Academy of Sciences of the United States of America*, *108*, 18843–18848. https://doi.org/10.1073/pnas.1105787108

Wainwright, C. E., Elborn, J. S., Ramsey, B. W., Marigowda, G., Huang, X., Cipolli, M., ... TRANSPORT Study Group (2015). Lumacaftor–ivacaftor in patients with cystic fibrosis homozygous for Phe508del CFTR. *The New England Journal of Medicine*, *373*, 220–231. https://doi.org/10.1056/NEJMoa1409547

Weiss, J. N. (1997). The Hill equation revisited: Uses and misuses. *The FASEB Journal*, *11*, 835–841. https://doi.org/10.1096/fasebj.11.11.9285481

Willumsen, N. J., Davis, C. W., & Boucher, R. C. (1989). Intracellular Cl^- activity and cellular Cl^- pathways in cultured human airway epithelium. *The American Journal of Physiology*, *256*, C1033–C1044. https://doi.org/10.1152/ajpcell.1989.256.5.C1033

Wu, X., Judd, L. W., Howe, E. N. W., Withecombe, A. M., Soto-Cerrato, V., Li, H., ... Gale, P. A. (2016). Nonprotonophoric electrogenic Cl^- transport mediated by valinomycin-like carriers. *Chem*, *1*, 127–146. https://doi.org/10.1016/j.chempr.2016.04.002

Zar, J. H. (1999). *Biostatistical analysis*. Englewood Cliffs, New Jersey: Prentice Hall.

Zegarra-Moran, O., & Galietta, L. J. V. (2017). CFTR pharmacology. *Cellular and Molecular Life Sciences*, *74*, 117–128. https://doi.org/10.1007/s00018-016-2392-x

SUPPORTING INFORMATION

Additional supporting information may be found online in the Supporting Information section at the end of the article.